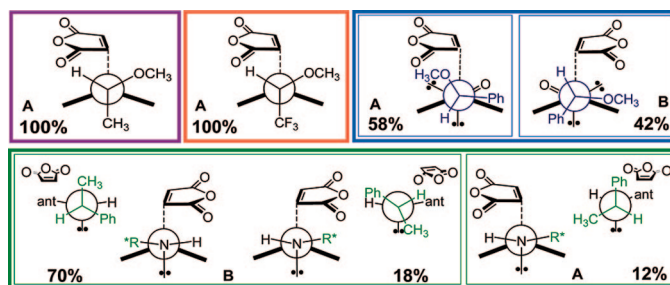# Understanding the Stereoselection Induced by Chiral Anthracene Templates in Diels−Alder Cycloaddition: A DFT Study

Nihan Çelebi-Ölçüm, Amitav Sanyal, and Viktorya Aviyente*

Department of Chemistry, Boğaziçi University, Bebek, Istanbul 34342, Turkey

aviye@boun.edu.tr

Received October 21, 2008

Recyclable chiral anthracene templates have emerged as an effective and well-designed approach in preparing complex biologically active molecules such as butenolides, α,β-unsaturated lactams, and related compounds in their enantiomerically pure forms. Highly diastereoselective initial cycloaddition serves as the key element of the total process, as it determines the final stereochemistry of the product. The diastereoselectivity of chiral anthracene templates is explored by using density functional theory (DFT) methods, and the reliability and applicability of the previously proposed models, mostly based on steric arguments, are tested by mechanistic means. The diastereomers **A** and **B** are identified according to the stereochemistry around the formed stereocenter on the dienophile attached to C9, as being *R* or *S*, respectively. The reactions of (*R*)-9-(1-methoxyethyl)anthracene and (*S*)-9-(1-methoxy-2,2,2-trifluoroethyl)anthracene with maleic anhydride both give exclusively diastereomer **A** via a similar transition state in which the CH_3/CF_3 group is antiperiplanar to the approaching dienophile. The major product of the reaction between (*R*)-9-(1-phenylethyl)aminoanthracene and maleic anhydride is diastereomer **B**. The geometry around nitrogen is close to planar in the transition state (10−25° out of plane), and the nitrogen lone pair is antiperiplanar to the incoming dienophile. Both of the lowest energy diastereomeric transition states giving **A** and **B** benefit from the favorable interaction between the carbonyl oxygen and the amine hydrogen; this interaction does not play a substantial role in the selectivity of the reaction as previously proposed. The diastereomeric transition states leading to **A** and **B** for the reaction between (*R*)-9-acyloxyanthracene and maleic anhydride have very similar interactions around the reaction center, leading to a very small energy difference between the diastereomeric transition states. The product distribution ratios for all templates calculated from Boltzmann distributions agree very well with the experimental results.

Introduction

One of the most common approaches in the synthesis of enantiomerically pure substances utilizes the concept of asymmetric induction.[1] The key idea is to form nonequivalent diastereomeric trajectories that selectively yield a single product.

This can be achieved by incorporating a stereocenter to the reagents or catalyst, for example, via use of chiral auxiliaries or chiral ligands. Among the chiral auxiliary based approaches, the use of chiral dienes as a "template" in asymmetric synthesis has emerged as an elegant and powerful methodology and has been applied toward the synthesis of numerous stereochemically complex molecules in their enantiomerically pure forms.[2] The methodology involves a Diels−Alder reaction of an achiral

(1) (a) Whitesell, J. K. *Acc. Chem. Res.* **1985**, *18*, 280−284. (b) Eliel, E. L.; Wilen, S. H.; Mander, L. N. *Stereochemistry of Organic Compounds*; Wiley: New York, 1994. (c) Koskinen, A. *Asymmetric Synthesis of Natural Products*; Wiley: New York, 1993. (d) Gnas, Y.; Glorius, F. *Synthesis* **2006**, 1899–1930. (e) Jacobsen, E. N., Pfaltz, A., Yamamoto, H., Eds. *Comprehensive Asymmetric Catalysis*; Springer: New York, 1999; Vols. I−III.

(2) Klunder, A. J. H.; Zhu, J.; Zwanenburg, B. *Chem. Rev.* **1999**, *99*, 1163–1190.

SCHEME 1. Stereoselective Functionalization of the Dienophile Using Chiral Anthracene Template
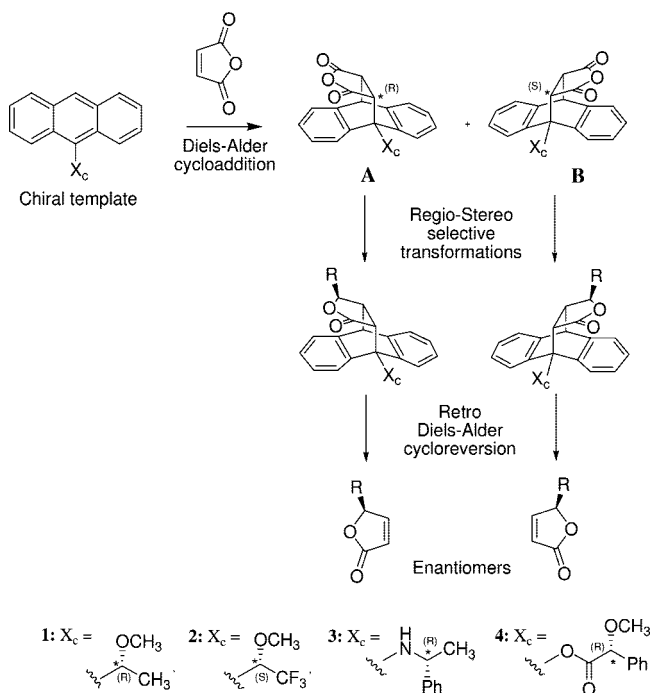
dienophile with the chiral diene to furnish a diastereomerically pure cycloadduct. Thereafter, the stereocenters on the cycloadduct allow stereocontrolled modifications of the dienophile subunit. Finally, a cycloreversion step regenerates the chiral diene template and releases the desired enantiopure product. One such strategy, developed by Snyder et al.[3−7] and Jones et al.[8−14] employs chiral anthracene templates in Diels−Alder/ retro-Diels−Alder sequences to stereoselectively functionalize the dienophile (Scheme 1). Biologically active substances such as butenolides, α,β-unsaturated lactams, and related compounds were successfully prepared from achiral dienophiles using chiral and recyclable anthracene templates with this strategy.[3−7] More recently, Liu and Snyder demonstrated that chiral anthracene based cycloadducts provide access to a valuable class of chiral auxiliaries that allow excellent diastereocontrol in a variety of reactions such as Diels−Alder cycloadditions, conjugate additions, and aldol reactions.[15] In this method, highly diastereoselective initial cycloaddition determines the final stereochem-

istry of the product (Scheme 1). So, much effort has been devoted to develop benchtop stable chiral anthracenes with improved reactivity and diastereoselectivity.[3−14]

The Diels−Alder reactions of several dienophiles with various chiral anthracene templates substituted at the C9 position with a stereogenic center have been extensively explored.[3−14] These cycloadditions can give two diastereomers, **A** and **B**, that can be identified with the stereocenter on the dienophile attached to C9 as being *R* or *S*, respectively. Exclusive diastereoselectivity has been successfully obtained with (*R*)-9-(1-methoxyethyl)anthracene (**1**) and (*S*)-9-(1-methoxy-2,2,2-trifluoroethyl)anthracene (**2**) when reacted with maleate derivatives.[3,5,8,10] Snyder and co-workers have then prepared anthracenes with electron-donating chiral substituents at the C9 position to obtain enhanced reactivity and cycloreversion at lower temperatures.[7] While (*R*)-9-acyloxyanthracene (**4**) has produced the diastereomers in a very low ratio (3:2), promising diastereoselectivity (>10:1) with (*R*)-9-(1-phenylethyl)aminoanthracene (**3**) together with improved reactivity has been achieved. Recent results of Adams et al.[14] supported the encouraging stereoselectivity obtained for **3**; however, they showed the stereochemical outcome of the reaction to be the opposite to that previously reported.
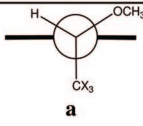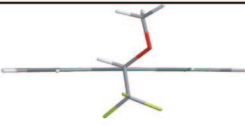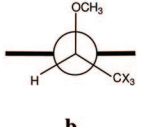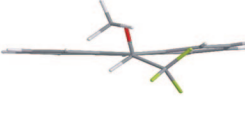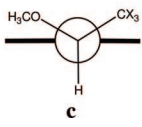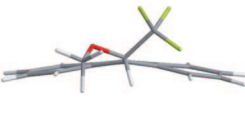
Asymmetric induction is usually explained by steric and electronic effects that determine the facial recognition. Steric interactions in the transition state can be used to derive models to predict the absolute stereochemistry of the products. When steric interactions are close to the reaction center, it is usually possible to explain the experimental outcome of the reaction with simple and reliable models based on steric arguments. This task is more demanding when the stereogenic center does not lie in the immediate proximity of the reaction center and even harder when the transition state is conformationally flexible. The degree of stereocontrol exerted by the chiral group depends on small energy differences between the diastereomeric transition state conformers and can easily be affected by minor changes.

Some models have already been proposed to explain the diastereoselectivity[3−14] of chiral anthracenes. The reaction of maleic anhydride (MA) with (*R*)-9-(1-methoxyethyl)anthracene (**1**) proceeding with exclusive diastereoselectivity has perhaps one of the most reliable models since the stereogenic center with well-known electronic characteristics is directly attached to the carbon involved in the bond formation process. However, the same model may not explain the product distribution when the electronic properties of the system are modified as in the case of compound **2**. Similarly, simple steric arguments are insufficient to explain the degree of stereocontrol caused by (*R*)-9-(1-phenylethyl)aminoanthracene (**3**) and (*R*)-9-acyloxyanthracene (**4**). In **3** and **4**, even though the location of the chiral center is more than one bond away from C9, there is a substantial difference in their experimental diastereoselectivities. Overall, the factors influencing the selectivities of Diels−Alder reactions of chiral fluoro-substituted anthracenes, aminoanthracenes, and acyloxyanthracenes require deeper mechanistic exploration.

In this study, we focus on the initial diastereoselectivity of the Diels−Alder cycloaddition and investigate the diastereoselection process of the chiral anthracene templates **1**, **2**, **3**, and **4** using density functional theory. We also examine the reliability of the previously proposed models. We first explore the reaction of MA with (*R*)-9-(1-methoxyethyl)anthracene (**1**) to validate our methodology and to provide a deeper insight into the

(3) Sanyal, A.; Snyder, J. K. *Org. Lett.* **2000**, *2*, 2527–2530.
(4) Corbett, M. S.; Liu, X.; Sanyal, A.; Snyder, J. K. *Tetrahedron Lett.* **2003**, *44*, 931–935.
(5) Burgess, K. L.; Lajkiewicz, N. J.; Sanyal, A.; Yan, W.; Snyder, J. K. *Org. Lett.* **2005**, *7*, 31–34.
(6) Burgess, K. L.; Corbett, M. S.; Eugenio, P.; Lajkiewicz, N. J.; Liu, X.; Sanyal, A.; Yan, W.; Yuan, Q.; Snyder, J. K. *Bioorg. Med. Chem.* **2005**, *13*, 5299–5309.
(7) Sanyal, A.; Yan, W.; Yuan, Q.; Snyder, J. K. *Tetrahedron Lett.* **2005**, *46*, 2475–2478.
(8) Jones, S.; Atherton, J. C. C. *Tetrahedron: Asymmetry* **2001**, *12*, 1117–1119.
(9) Atherton, J. C. C.; Jones, S. *Tetrahedron Lett.* **2001**, *42*, 8239–8241.
(10) Atherton, J. C. C.; Jones, S. *J. Chem. Soc., Perkin Trans. 1* **2002**, 2166–2173.
(11) Atherton, J. C. C.; Jones, S. *Tetrahedron Lett.* **2002**, *43*, 9097–9100.
(12) Adams, H.; Jones, S.; Ojea-Jimenez, I. *Org. Biomol. Chem* **2006**, *4*, 2296–2303.
(13) Adams, H.; Bawa, R. A.; Jones, S. *Org. Biomol. Chem.* **2006**, *4*, 4206–4213.
(14) Adams, H.; Bawa, R. A.; McMillan, K. G.; Jones, S. *Tetrahedron: Asymmetry* **2007**, *18*, 1003–1012.
(15) Liu, X.; Snyder, J. K. *J. Org. Chem.* **2008**, *73*, 2935–2938.

TABLE 1. NBO Analysis of the Conformers of 1 and 2[a]

Conformation	1 (X=H)			2 (X=F)			3 Structure[i]
	ΔE_{el}	$\Delta E_{(L)}$	$\Delta E_{(NL)}$	ΔE_{el}	$\Delta E_{(L)}$	$\Delta E_{(NL)}$	
a	0.0	0.0	0.0	0.0	0.0	0.0	
b	8.0	5.5	2.5	7.4	4.8	2.6	
c	11.3	2.9	8.4	15.2	7.8	7.4	

[a] Relative electronic energies (ΔE_{el}), Lewis ($\Delta E_{(L)}$), and non-Lewis ($\Delta E_{(NL)}$) contributions to the electronic energies (kcal/mol). [i] 3D structures for **1** are given in the Supporting Information.

stereoelectronic features of the transition states leading to the diastereomers. We then model the reaction of MA with (S)-9-(1-methoxy-2,2,2-trifluoroethyl)anthracene (**2**). As such, the aim is to understand the selectivity of similar systems but with very different electronic properties. Finally, we focus our attention to the reactions of MA with (R)-9-(1-phenylethyl)aminoanthracene (**3**) and (R)-9-acyloxyanthracene (**4**) giving two diastereomeric products **A** and **B**, with very different diastereoselectivities that cannot be explained by simple steric models.

Computational Methodology

All DFT calculations were carried out with Gaussian 03.[16] The Becke three-parameter exchange functional and the nonlocal correlation functional of Lee, Yang, and Parr (B3LYP) have been employed with the 6-31+G(d) basis set. Geometry optimizations were performed for all reactants, transition states, and products. Frequency calculations were used to characterize the stationary points as minimum or saddle point and to provide thermal and zero point corrections. Gas phase enthalpies are reported throughout the text unless otherwise specified. The minimum energy paths were followed by the intrinsic reaction coordinate method (IRC).[17] Solvent effects were considered using the IEFPCM methodology with the UA0 cavity model as implemented in Gaussian 03. Toluene is used as the solvent to represent the experimental conditions. Free energies and solvent energies are given in the Supporting Information.

The conformational space was initially explored systematically with 3-fold rotation around the single bonds using the semiempirical PM3 method. The conformers within 3 kcal/mol energy range were then optimized with B3LYP/6-31+G(d) to get a more accurate description of the conformer distribution. Single point energies of these conformers in toluene were calculated. For **1** and **2**, an additional relaxed potential energy surface scan was performed with 60° increments around the C9–C* bond atom at the B3LYP/6-31+G(d) level of theory.

Natural bond orbital analysis (NBO) was performed on the conformers of **1** and **2**.[18−22] The role of electronic delocalizations was quantitatively assessed by deleting all non-Lewis NBOs from the basis set. The net energy difference between the original electronic energy (E_{el}) and the energy of the perfectly localized Lewis-type wave function ($E_{(L)}$) gives the electronic delocalization energy ($E_{(NL)}$) and describes the stabilizing effect of the delocalizing (non-Lewis) contributions (eq 1).

$$E_{(NL)} = E_{el} - E_{(L)} \qquad (1)$$

To understand specific interactions responsible for the conformational preferences, all hyperconjugative delocalizations between "filled" (donor) Lewis-type NBOs and "empty" (acceptor) non-Lewis NBOs were examined and their energetic importance was estimated by second-order perturbation theory. It has been shown that the use of diffuse functions in NBO calculations leads to erroneous results originating from the augmented Rydberg orbital's extension.[23] The NBO calculations were, therefore, performed by using the B3LYP methodology and 6-31G(d) basis set, and the electronic energies are reported in the text.

Results and Discussion

Reactions of (R)-9-(1-Methoxyethyl)anthracene (1) and (S)-9-(1-Methoxy-2,2,2-trifluoroethyl)anthracene (2) with MA. The conformational analysis of **1** and **2** has shown a strong energetic bias toward structures in which the methyl and trifluoromethyl groups on the stereogenic center occupy a position perpendicular to the anthracene plane. This conformational preference is justified by a relaxed potential energy surface scan around the bond connecting C9 with the chiral carbon atom (C9–C*).

The conformations obtained from the PES scan (**a**, **b**, and **c**) have been analyzed to understand the factors contributing to

(16) Frisch, M. J.; et al. *Gaussian 03*, revision D.01; Gaussian, Inc.: Wallingford CT, 2004.
(17) (a) Gonzalez, C.; Schlegel, H. B. *J. Chem. Phys.* **1989**, *90*, 2154–2161. (b) Gonzalez, C.; Schlegel, H. B. *J. Phys. Chem.* **1990**, *94*, 5523–5527.

(18) Foster, P.; Weinhold, F. *J. Am. Chem. Soc.* **1980**, *102*, 7211–7218.
(19) Reed, A. E.; Weinhold, F. *J. Chem. Phys.* **1983**, *78*, 4066–4073.
(20) Reed, A. E.; Weihstock, R. B.; Weinhold, F. *J. Chem. Phys.* **1985**, *83*, 735–746.
(21) Foster, P.; Weinhold, F. *J. Chem. Phys.* **1985**, *83*, 1736–1740.
(22) Reed, A. E.; Curtiss, L. A.; Weinhold, F. *Chem. Rev.* **1988**, *88*, 899–926.
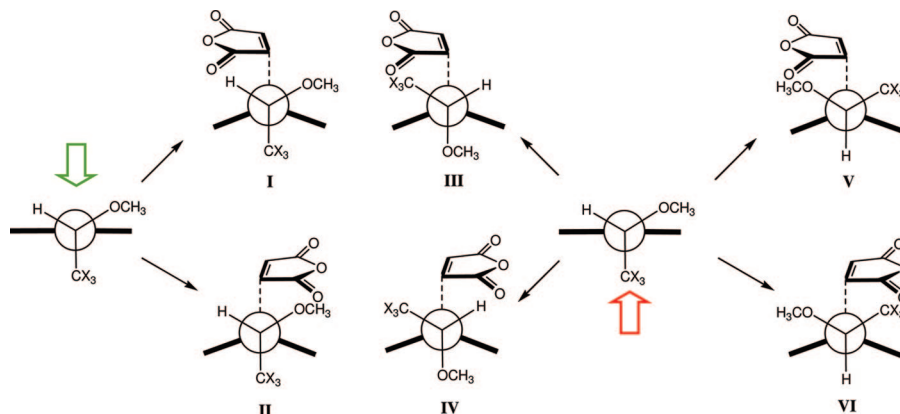(23) Goodman, L.; Sauers, R. *J. Comput. Chem.* **2006**, *28*, 269–275.

FIGURE 1. Model transition states leading to diastereomers **A** and **B** for the reactions between **1** (X = H) and MA and **2** (X = F) and MA.

the stabilization of **1a** and **2a** (Table 1). In structures **1a** and **2a**, the anthracene ring is completely planar. The significant distortions of the anthracene ring in structures **1b**, **2b**, **1c**, and **2c** can be accounted for by the steric repulsions between the anthracene ring and the bulky *syn* substituents. The localized $E_{(L)}$ contributions strongly favor **1a** and **2a**, in accordance with the expected steric and electrostatic effects. Energy differences between conformers are further amplified by the delocalization contributions $\Delta E_{(NL)}$. **1c** is 2.6 kcal/mol lower in energy than **1b** in the absence of electronic delocalizations, and this difference can be attributed to an electrostatically more favorable arrangement of the methyl and methoxy groups ($\Delta E_{(L)}$ (**1b**) = 5.5 kcal/mol, $\Delta E_{(L)}$ (**1c**) = 2.9 kcal/mol). However, **1b** is highly stabilized by the electronic delocalization energy and favored overall by 3.3 kcal/mol as compared to **1c** ($\Delta E_{(NL)}$ (**1b**) = 2.5 kcal/mol, $\Delta E_{(NL)}$ (**1c**) = 8.4 kcal/mol). In the case of compound **2**, the electrostatic repulsions between the trifluoromethyl and methoxy groups destabilize **2c** by 3.0 kcal/mol as compared to **2b** when electronic delocalizations are not taken into account ($\Delta E_{(L)}$ (**2b**) = 4.8 kcal/mol, $\Delta e_{(l)}$ (**2c**) = 7.8 kcal/mol). **2c** is further disfavored by lack of delocalizations, leading to very large total energy differences with **2a** and **2b** ($\Delta E_{(NL)}$ (**2b**) = 2.6 kcal/mol, $\Delta E_{(NL)}$ (**2c**) = 7.4 kcal/mol). The stability of **1c** relative to **2c** ($\Delta\Delta E_{el}$ = 3.9 kcal/mol) can be explained by the differences in the electrostatic interactions between the substituents, whereas the relative energies of **1b** and **1c** are very close ($\Delta\Delta E_{el}$ = 0.6 kcal/mol) due to similar Lewis and non-Lewis contributions.

To understand specific interactions responsible for the energy difference, hyperconjugative delocalizations involving the acceptor and donor NBOs on the chiral carbon (CH, $CC_{(CX3)}$, and CO) are explored in detail. The most important contributions to the stabilization of **a** compared to both **b** and **c** is found to be the vicinal hyperconjugative interactions between the donor/acceptor $CC_{(CX3)}$ NBOs on the chiral carbon with the acceptor/donor OC NBOs on the methoxy group that shows a favorable antiperiplanar arrangement in **a** (see Supporting Information). The hyperconjugative interactions between the anthracene aromatic system and the CH, $CC_{(CX3)}$, and CO antibonds on the chiral carbon give an extra stabilization of about 2.5 kcal/mol to both **a** and **b** as compared to **c**. A detailed list of donor−acceptor interactions and their stabilization energies are given in the Supporting Information.

Figure 1 shows model transition states leading to diastereomers **A** and **B** for the cycloadditions of MA with **1** and **2**. When MA approaches from the face opposite to the CH$_3$/CF$_3$ group, the diastereoselection occurs between **I** and **II**. The approach

of MA from the face hindered by the CH$_3$/CF$_3$ groups results in the transition state models **III**, **IV**, **V**, and **VI**.

In Figure 2, transition state conformers yielding diastereomers **A** and **B** are shown. Charge distributions and distances between repulsive and attractive centers are also displayed. Even though the strength of CH−O interactions cannot be solely predicted based on the CH···O distances, especially in gas phase optimized geometries, assessment of such interactions may pave the way for rationalizing the relative stabilities of the alternative transition state conformations.

The most stable transition state for the reaction between **1** and MA, **TS1-I**, leads to **A** with an activation enthalpy of 19.9 kcal/mol. In this transition state, the carbonyl oxygen fits into the hydrogen pocket. The charge distribution reveals an electrostatically more favorable arrangement compared to the other transition state alternatives given in Figure 2. The methoxy oxygen favorably interacts with the hydrogen on MA (2.49 Å) and the hydrogen on the bent anthracene (2.31 Å). The carbonyl oxygen on MA seems to be stabilized mostly by the hydrogen atom on the stereogenic center (2.60 Å) and on the methoxy substituent (2.83 Å). The minimum energy transition state leading to diastereomer **B**, **TS1-IV**, is 3.6 kcal/mol above **TS1-I**. The carbonyl moiety also nicely fits into the hydrogen pocket, although at a larger distance (2.99 Å) than in the previous case (2.60 Å). The methyl group of the methoxy is tilted toward the hydrogen on the stereogenic center in order to avoid steric repulsions between the two large methyl groups. **TS1-II** also leads to **B** but is 0.9 kcal/mol higher in energy than **TS1-IV**. It suffers from electrostatic repulsion between the oxygens, although the oxygen of the methoxy group interacts favorably with the hydrogen on the antharacene ring (2.24 Å). **TS1-III** has an activation enthalpy of 26.1 kcal/mol and is the most asynchronous transition state with destabilizations due to repulsive steric interactions. **TS1-V** and **TS1-VI** are strongly destabilized by both steric and electrostatic repulsions of the methyl and the methoxy groups with the anthracene ring, similar to the repulsions in **1c**, and have high activation enthalpies, 29.4 and 28.9 kcal/mol, respectively.

TS1-I, the lowest energy transition state, gives **A** as the major product. The origin of the experimentally observed exclusive selectivity in the reaction between **1** and MA stems from the difference in the activation enthalpies between **TS1-I** and **TS1-IV**.

It is possible to alter the electronic features of the chiral anthracene template simply by changing the hydrogens on the electron-donating methyl group with highly electronegative fluorine atoms. As such, a high electron density region is
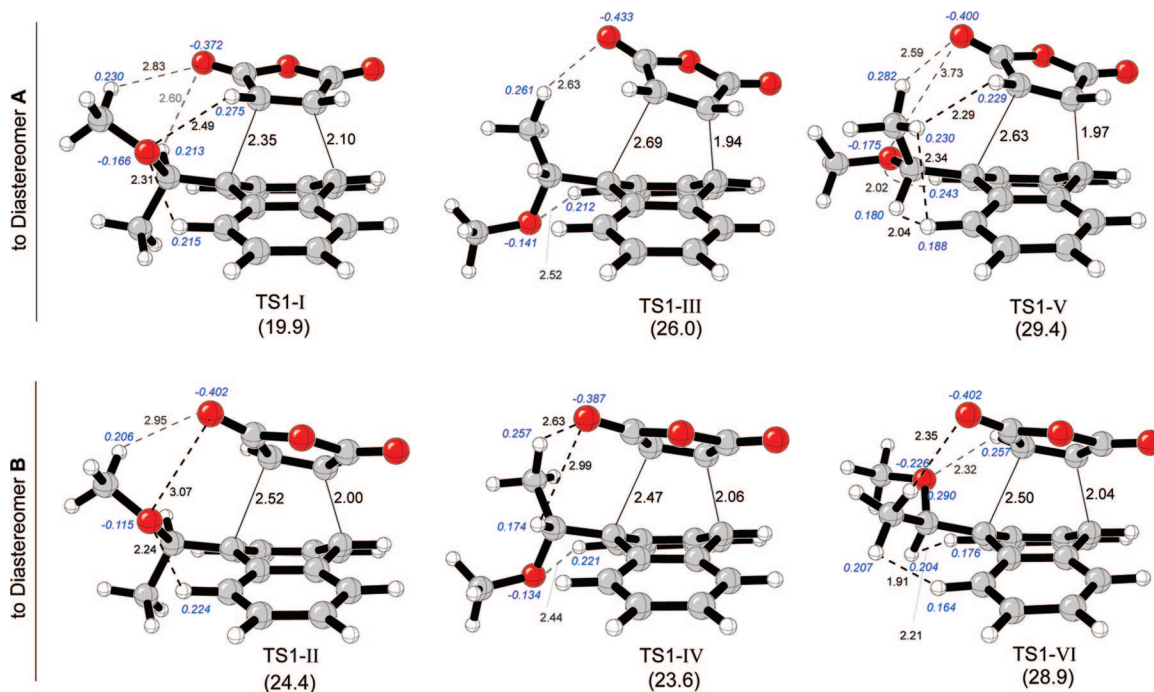
FIGURE 2. Transition states corresponding to transition state models **I**−**VI** for the reaction of MA with **1**. The values in parentheses are the activation enthalpies ($\Delta H^{\ddagger}$) in kcal/mol. Mulliken charges of the interacting atoms are given in italics.
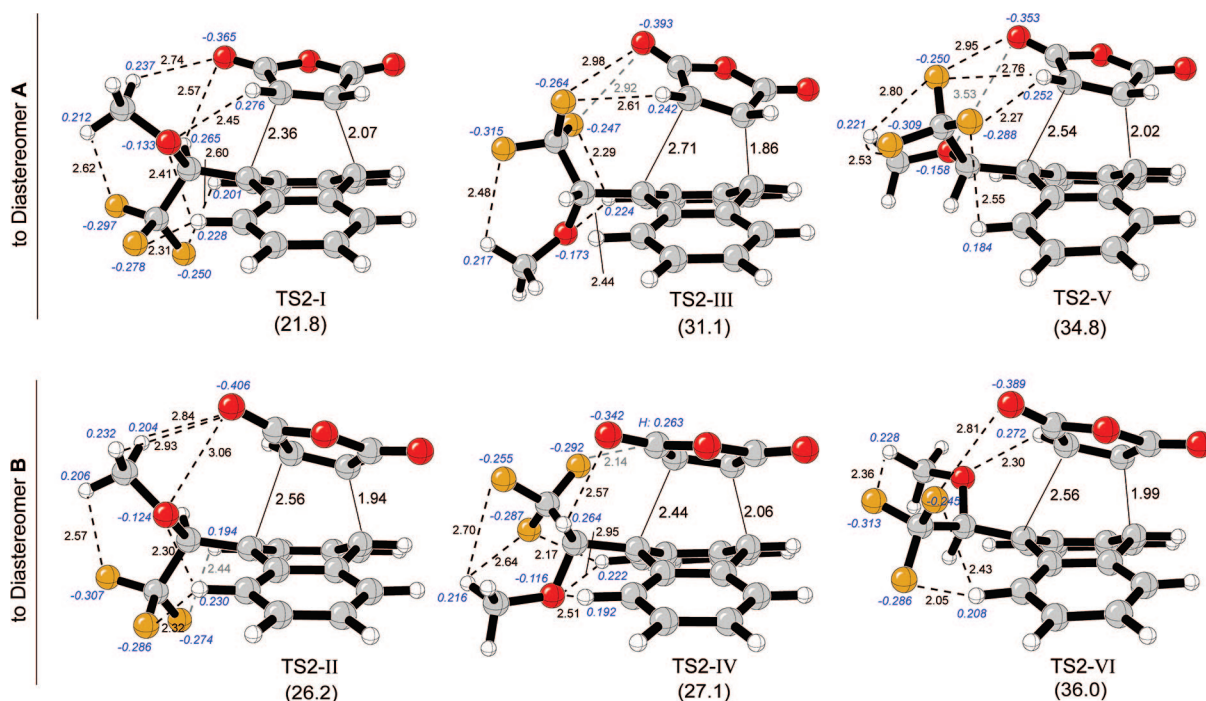

FIGURE 3. Transition states corresponding to transition state models **I**−**VI** for the reaction of MA with **2**. The values in parentheses are the activation enthalpies ($\Delta H^{\ddagger}$) in kcal/mol. Mulliken charges of interacting atoms are given in italics.

introduced next to the reaction center. The electron-withdrawing trifluoromethyl group is well-known to exhibit unusual steric effects attributed to the very large effective negative charge it carries. Accordingly, with **2**, the transition state model **V**−rather than **I**−has been proposed to explain the obtained diastereoselectivity of the reaction.[4]

Figure 3 summarizes the transition states, activation enthalpies, as well as favorable and unfavorable electrostatic interactions in the transition states for the reaction between **2** and MA. The lowest energy transition state is again obtained from model

I that yields **A** as the product. The activation enthalpy of **TS2-I** is 21.8 kcal/mol, 1.9 kcal/mol higher enthalpy barrier compared to **TS1-I**. This fact can be rationalized by the electron-withdrawing character of the CF$_3$ substituent on the diene. In **TS2-I**, MA approaches *syn* to the hydrogen and the methoxy group and the carbonyl group nicely fit into the pocket of the small hydrogen atom. The approach of MA in **TS2-I** not only prevents the steric and electrostatic repulsions but also accounts for a large number of favorable electrostatic interactions. The hydrogen on the stereogenic center and the carbonyl oxygen

seem to interact favorably (2.57 Å). The electronegative fluorine atoms are squeezed between the partially positively charged hydrogens on the bent anthracene ring (2.31 and 2.60 Å). The hydrogen on MA and the hydrogen on the anthracene ring interact favorably with the methoxy oxygen (2.45 and 2.30 Å), while the hydrogen on the methoxy group electrostatically stabilizes the electron-rich fluorine atom (2.62 Å).

TS2-IV is a potential transition state yielding **B** with no unfavorable electrostatic interactions. **TS2-II** also yields **B** as the product, but it suffers from electrostatic repulsions between the lone pairs of the methoxy oxygen and the carbonyl oxygen. Despite this destabilizing interaction, **TS2-II** is stabilized with respect to **TS2-IV** by 1 kcal/mol, presumably because of the repulsive interactions between the electron density on the dienophile and the one around CF_3 in the former. **TS2-II** is 4.4 kcal/mol higher in energy than **TS2-I**. The electrostatic repulsion between the oxygens is partly diminished by the favorable interaction between the oxygen on the methoxy group and the hydrogen on the anthracene ring (2.30 Å). Electrostatic stabilizing interactions between the fluorine atom and the hydrogen on the methoxy substituent can also be expected (2.57 Å). The electronegative fluorine atoms also favorably interact with the hydrogens of the bent anthracene (2.32 and 2.44 Å).

The activation enthalpy for **TS2-IV** is 27.1 kcal/mol. The electronegative fluorine atoms are stabilized by the hydrogen on MA and the hydrogen on the anthracene ring (2.17 and 2.13 Å). As in **TS2-I**, there seems to be a stabilizing interaction between the carbonyl oxygen and the hydrogen on the stereogenic center (2.57 Å). The lone pairs of the methoxy oxygen interact favorably with the hydrogen on the anthracene ring (2.51 Å) and the methoxy hydrogen interacts with two fluorine atoms on CF_3 (2.70 Å, 2.64 Å). Although there seems to be no unfavorable interaction between the diene and the dienophile in **TS2-IV**, the number of stabilizing interactions is smaller as compared to the ones in **TS2-I**, and the high electron density region around CF_3 unfavorably interacts with the negative charge on the dienophile.

TS2-III yields **A** and is destabilized by 9.5 kcal/mol as compared to **TS2-1**. There are large steric and electrostatic repulsions between the oxygen lone pairs and the highly electronegative fluorine atoms. In **TS2-V**, the dienophile is *syn* to the CF_3 and the OCH_3 substituents and *anti* to the hydrogen. This model has been previously proposed to explain the observed stereoselectivity of the reaction. According to Corbett et al.,[4] **2** at a conformation with the hydrogen perpendicular to the anthracene plane (**2c**) should be the most reactive conformer. In this conformation, maximum σ-donation due to the alignment of the relatively acidic C−H bond of the stereogenic center with the anthracene orbitals has been anticipated, raising the HOMO$_{diene}$. The dienophile is suggested to approach **2c** as in model **V** to avoid the stronger electrostatic repulsion of the CF_3 group as compared to the neighborhood of the methoxy oxygen. However, the conformational analysis results have shown that, starting from the minimum energy conformer **2a**, the energy increases gradually as rotation around the C9−C* bond proceeds: **2c** is 15.2 kcal/mol higher in energy than **2a** (see Table 1) Thus, the frontier orbitals cannot be used to set up a reliable model as claimed earlier.[4] As expected, the optimized transition state geometry, **TS2-V**, is found to be much higher in energy than the transition states obtained from models **I**−**IV**.

The activation enthalpy of **TS2-V** is 34.8 kcal/mol. It contains only a few favorable electrostatic contacts, all between the fluorine atoms and the hydrogens. One fluorine atom interacts with the hydrogen on MA and the hydrogen on the bent anthracene (2.27 and 2.55 Å); the hydrogen on MA also interacts with another fluorine atom (2.74 Å), and the hydrogen of the methoxy group interacts with two fluorine atoms (2.53 and 2.80 Å).

TS2-VI leads to **B** with an activation enthalpy of 36.0 kcal/mol. Despite the seemingly favorable electrostatic interactions between the hydrogen on MA and the methoxy oxygen (2.30 Å), the hydrogen on the bent anthracene with two fluorine atoms (2.43 and 2.05 Å), and the hydrogen on the methoxy group with the fluorine atom (2.36 Å), this transition state is 14.6 kcal/mol higher than **TS2-I**. Unfavorable steric contacts cause a large destabilization. The highest electron density regions of the diene and the dienophile are in very close contact, contributing to the expected high energy barrier.

As confirmed by the calculations in the gas phase and in toluene, the exclusive product of the reaction is **A**. The reaction proceeds through the transition state model **I**. **TS2-I** is 1.9 kcal/mol higher in energy than **TS1-I**, in accordance with the experimentally observed rate deceleration. The building negative charge on the dienophile and the high effective negative charge around the CF_3 group unfavorably interact and lead to higher activation enthalpies when the dienophile is *syn* to the CF_3 group.

Reaction of (*R*)-9-(1-Phenylethyl)aminoanthracene (3) with MA. In **3**, the electron-donating chiral amino group attached to the anthracene ring is expected to increase the rate of the reaction.[7] The diastereoselectivity of the reaction is found to be interestingly high although the stereogenic center was not in the immediate proximity of the reaction center. Adams et al.[14] have identified **B** as the major product by X-ray crystallography.

Amines with three different but independent R groups do not show chirality due to rapid Walden inversion around nitrogen. Compound **3** is found to be present in two dominating conformations, **3a** and **3b**. The optimized geometries of **3a** and **3b** are shown in Figure 4. In both conformers, the amine hydrogen and the hydrogen on the stereogenic center prefer to occupy *anti* positions to each other. In **3a**, the phenyl group points away from the anthracene ring, whereas in **3b**, the phenyl group points toward the anthracene ring. The crystal structure obtained by Adams et al.[14] strongly agrees with conformer **3b**. The enthalpy difference between **3a** and **3b** is found to be only 0.8 kcal/mol in the gas phase. The difference between their energies in toluene is as low as 0.1 kcal/mol, indicating that a diastereomeric mixture is present in the reaction medium (see Supporting Information).

Adams et al.[14] have proposed that the diastereoselection occurs as the dienophile approaches the anthracene ring *anti* to the chiral carbon in two different ways. In the favored approach, the carbonyl oxygen is oriented toward the amine hydrogen and in the disfavored approach the carbonyl oxygen is oriented toward the nitrogen lone pair. As such, they underlined the importance of a combination of electrostatic repulsion and attractive hydrogen bonding in establishing high levels of diastereoselectivity, giving **B** as the major product. This model, however, is based on the assumption that a single conformation dominates over the other and fails to explain the product distribution in the presence of both **3a** and **3b**. As shown in Figure 5, a mixture of **3a** and **3b** would favorably yield both **A** and **B**, contradicting the observed levels of diastereoselectivity. It has also been assumed that the most stable conformation of the chiral anthracene template is maintained in the transition state. In fact, a conformation with the stereodirecting group *syn*
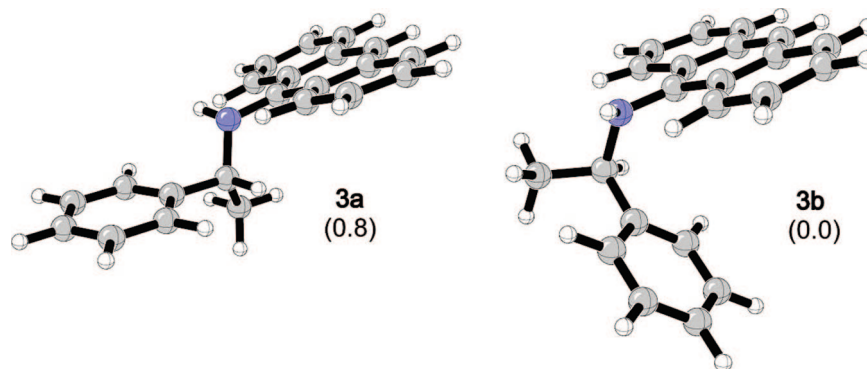
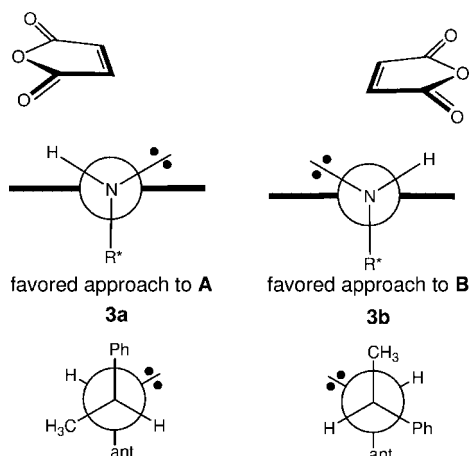FIGURE 4. Conformers of 3. The values in parentheses are the relative enthalpies in kcal/mol.

FIGURE 5. Favored approaches of MA to 3a and 3b as proposed by Adams et al.[14] and the Newman projections of 3a and 3b through the stereogenic carbon atom to the nitrogen.
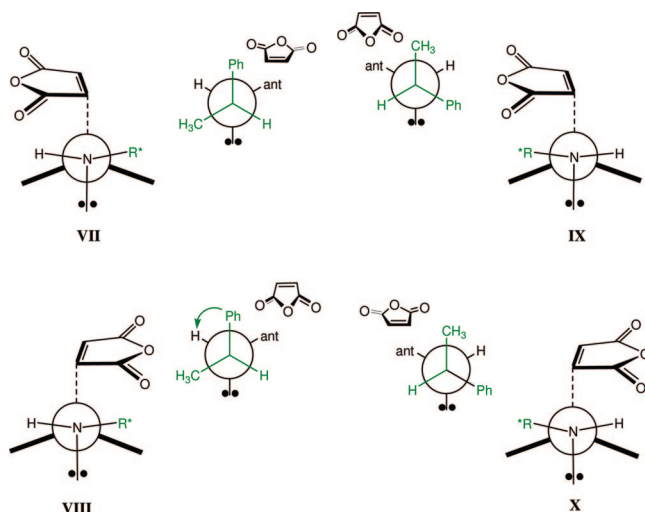

FIGURE 6. Model transition states leading to diastereomers A and B for the reaction between MA and 3.

and the nitrogen lone pair *anti* to the dienophile in the transition state may lead to a better stabilization and a more pronounced stereocontrol exerted by the chiral group.

We, therefore, propose transition state models VII–X (Figure 6), in which the nitrogen lone pair is *anti* to the dienophile. The free rotation around the C–N bond can additionally assist to diminish the unfavorable steric interactions. In model VIII, for example, the phenyl group can rotate toward the amine hydrogen to diminish the electrostatic repulsions with the carbonyl oxygen.

Optimized transition state geometries shown in Figure 7 have confirmed the suggested models (VII–X). All calculated structures predict that the lone pair on nitrogen is *anti* to MA and the geometry around nitrogen is close to planar (10–25° out of plane). Attempts to locate transition states with a nitrogen lone pair *syn* to MA as proposed by Adams et al. resulted in structures TS3-VII to TS3-X.

The lowest activation barrier is predicted for TS3-X (14.8 kcal/mol), and the IRC path connects the reactants to B, in agreement with the results of Adams et al.[14] The activation enthalpy of this transition state is 5.1 kcal/mol lower than TS1-I. The lower activation enthalpies for the reaction of chiral amino anthracene (3) and MA can be attributed to the electron donor character of the amine group attached to the diene. However, the energy differences giving rise to stereoselectivity are not high; the chiral center is not close to the reaction site, resulting in weaker steric and electrostatic effects. TS3-VIII and TS3-X both lead to B; in the former, the carbonyl group is in the pocket hindered by the chiral group instead of favorably interacting with the amine hydrogen. The loss of stabilization due to this interaction is only 0.8 kcal/mol.

TS3-IX yields A and has the highest activation enthalpy (18.2 kcal/mol). In contrast to the other alternative transition states, there is no interaction between the dienophile and the aromatic hydrogens of the phenyl ring in TS3-IX, suggesting the importance of this interaction in stabilizing a transition state conformation. Increased asynchronicity and steric effects also contribute to the destabilization of this transition state. The other transition state giving A, TS3-VII, is 2.4 kcal/mol lower in energy than TS3-IX; however, it is still 1.0 kcal/mol higher in energy than the most stable transition state, TS3-X, leading to B. Although in TS3-VII the carbonyl oxygen interacts favorably with the hydrogen on the amino group, its energy is comparable to TS3-VIII, which lacks this interaction.

All located transition states are very asynchronous; the forming C–C bond next to the chiral amino substituent is 2.8–3.0 Å, as the other forming C–C bond is about 2.0 Å. Hydrogen bonding is found to have no considerable effect on the diastereoselection process since both of the lowest energy transition states leading to A and B benefit from this interaction. In TS3-VII, the distance between carbonyl oxygen and amine hydrogen is 2.76 Å, whereas in the lowest energy transition state, TS3-X, it increases to 2.90 Å. The crystal structures of the major and minor products reported by Adams et al.[14] agree very well with the products of TS3-X and TS3-VII obtained from IRC calculations (see the Supporting Information for the geometries of products) and show the hydrogen attached to the amino group interacting with the carbonyl oxygen in both of
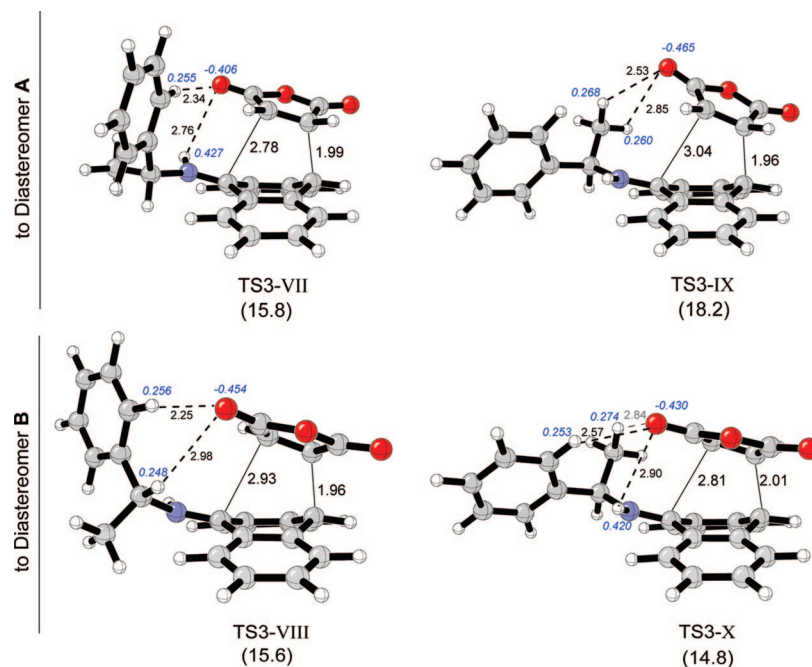
FIGURE 7. Transition states for the reaction of MA with **3**. The values in parentheses are the activation enthalpies ($\Delta H^{\ddagger}$) in kcal/mol. Mulliken charges of interacting atoms are given in italics.
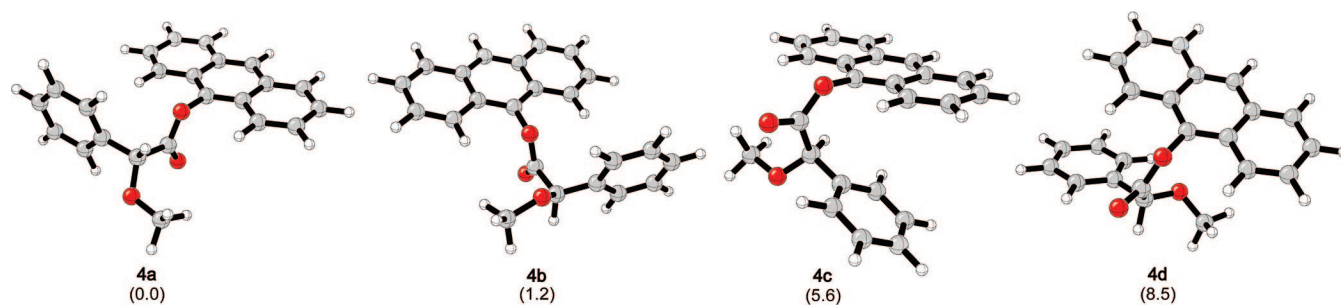

FIGURE 8. Minimum energy conformations of **4**. The values in parentheses are the relative enthalpies (ΔH) in kcal/mol.

the structures. In transition states **TS3-VII**, **TS3-VIII**, and **TS3-X**, the *ortho* hydrogen on the phenyl substituent interacts with the oxygen on the carbonyl group (2.34, 2.57, and 2.25 Å). In **TS3-IX**, the negative charge on the carbonyl oxygen is stabilized by the methyl hydrogens (2.53 and 2.85 Å).

The major product of the reaction is predicted to be **B** with two low energy transition states **TS3-X** and **TS3-VIII** giving this product. The lowest energy transition state yielding **A** is 1.0 kcal/mol higher in energy than **TS3-X**. In all transition states, the nitrogen lone pair is *anti* to the dienophile. Hydrogen bonding has no substantial effect on the obtained diastereoselectivity since both of the transition states leading to the diastereomeric products benefit from this interaction. The calculated product distribution ratio (B/A 88:12 in gas phase and 96:4 in toluene) agrees well with the experimental results (B/A 91:9).

Reactions of (*R*)-9-Acyloxyanthracenes with MA. *O*-Methylmandelic acid has been successfully employed by Trost and co-workers[24] as a covalent chiral auxiliary in the Diels—Alder reactions of their dienol esters to give moderate to high diastereoselectivities, despite the fact that the stereogenic center is located three bonds away from the site of bond formation. (*R*)-9-Acyloxyanthracene (**4**), however, gave very low diastereoselectivity

in the cycloaddition process. The low diastereoselectivity of **4** also contrasts the remarkable diastereoselectivities obtained with chiral amino anthracene **3**. This selectivity difference cannot be rationalized with simple steric arguments because in both of the compounds the stereogenic center is more than one bond away from the reaction center. Even though it has been suggested that hydrogen bonding can provide a diastereoselective improvement in **3** as compared to **4**,[14] our results have shown that the hydrogen bonding between the diene and the dienophile in **3** had no effect on the diastereoselection process.

4 is a highly flexible substrate with five rotatable bonds. The conformational preferences of **4** are shown in Figure 8. **4a** and **4b** are found to be the dominating conformers in the gas phase and in toluene (see Supporting Information). In the minimum energy conformer **4a**, the phenyl group is perpendicular to the anthryl group, with one face toward the anthracene ring. The carbonyl and the methoxyl oxygens are in an eclipsed arrangement as shown previously for α-alkoxy esters.[25] However, the dienyl and carboxyl groups are perpendicular to each other due to the steric constraints imposed by the anthracene ring rather than being in a co-planar arrangement as reported for the dienol esters of *O*-methylmandelic acid.[25] **4b** is 1.2 kcal/mol higher in energy than **4a** in the gas phase

(24) Trost, B. M.; O'Krongly, D.; Belletire, J. L. *J. Am. Chem. Soc.* **1980**, *102*, 7595–7596.

(25) Tucker, J. A.; Houk, K. N.; Trost, B. M. *J. Am. Chem. Soc.* **1990**, *112*, 5465–5471.
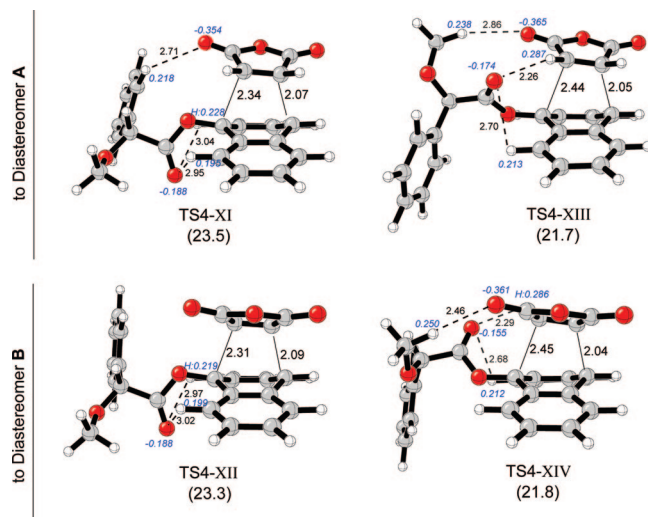
FIGURE 9. Transition states for the reaction of MA with **4**. The values in parentheses are the activation enthalpies ($\Delta H^{\ddagger}$) in kcal/mol. Mulliken charges of interacting atoms are given in italics.

and 1.0 kcal/mol in toluene (see Supporting Information). In **4b**, the carbonyl group is eclipsed to the CH bond instead of the methoxy oxygen. Two other conformers (**4c** (+5.6 kcal/mol) and **4d** (+8.5 kcal mol)), where the phenyl ring and the anthracene ring are face to face, have also been located.

To be able to explain the low diastereoselectivity of **4**, we located the transition states of the cycloaddition process between **4** and MA. The relative activation enthalpies of the transition states (Figure 9) show that the diastereoselection occurs between **TS4-XIII** and **TS4-XIV**. The arrangement of the dienophile in these transition states allows the stabilization of the hydrogen on MA with the carbonyl oxygen on the template. This favorable interaction stabilizes **TS4-XIII** and **TS4-XIV** by about 2 kcal/mol as compared to the transition states obtained from the *syn* approach to the oxygen lone pairs (**TS4-XI** and **TS4-XII**). However, the energy difference between **TS4-XIII** and **TS4-XIV** is very small ($\Delta H^{\ddagger}$ = 21.7 and 21.8 kcal/mol, respectively), in agreement with the observed low levels of diastereoselectivity.[7] The geometries of these two transition states are very similar, especially around the reaction center. In both transition states, the carbonyl oxygen on the anthracene template is tilted toward the hydrogen on MA, taking advantage of the stabilizing electrostatic attraction between the negatively charged oxygen and the positively charged hydrogen (2.29 and 2.26 Å) and also interacts favorably with the hydrogen on the bent anthracene ring (2.68 and 2.70 Å). The hydrogen on the methoxy substituent interacts with the carbonyl oxygen on MA (2.46 and 2.86 Å).

TS4-XI and **TS4-XII**, on the other hand, have higher activation enthalpies, ($\Delta H^{\ddagger}$ = 23.5 and 23.3 kcal/mol, respectively) and less favorable interactions. The carbonyl oxygen on MA interacts with the *ortho* hydrogen on the phenyl substituent in **TS4-XI** (2.71 Å). The carbonyl group is favorably squeezed between the hydrogens on the bent anthracene in **TS4-XI** (3.04 and 2.95 Å) and in **TS4-XII** (2.97 and 3.02 Å).

In the lowest energy conformations of **4**, the carboxyl and the anthryl groups are in a perpendicular arrangement and MA preferably attacks **4** from the face of the carboxyl group. This

attack allows the favorable interaction between the carbonyl oxygen on the acyloxyanthracene and the hydrogen on MA in both of the diastereomeric transition states. The interactions around the reaction site are very similar, leading to a very small energy difference between the diastereomeric transition states. This can originate from the conformational differences around the stereogenic center.

The calculated product distribution ratios (A/B 57:43 in gas phase and 64:36 in toluene) are in close agreement with the experimentally observed low diastereoselectivity (A/B 60:40) (see Supporting Information).

Conclusion

For substrates with high degrees of rotational freedom and flexible chiral groups, models based on the conformations of the reactants and related facial recognition may not be sufficient to determine the most favorable transition state conformation and thus the selectivity. The arguments based on frontier molecular orbital theory and facial recognition due to stereo-electronic effects have to be dealt with care. Eventually, a thorough analysis of the transition state conformations leading to each diastereomer is necessary in order to elucidate the selectivity of the reaction.

For the reactions of chiral anthracenes **1−4** with MA, our results have shown that **1** and **2** exclusively give **A** via a similar transition state in which the CH₃/CF₃ group is *anti* to the dienophile. The high diastereoselectivity obtained with **3** is found to depend on the stereoelectronic effects of the chiral substituent rather than the hydrogen bonding between the dienophile and the amine hydrogen on C9 of the diene. The loss of dieastereoselectivity in **4** can be based on the presence of similar interactions—favorable interaction of the carbonyl group on the diene with the hydrogen on MA—around the reaction center in both diastereomeric transition states. The calculated product distributions in the gas phase and in toluene are in very close agreement with the experimental results (see Supporting Information).

The experimentally observed rate deceleration for the cycloaddition of **2** is well predicted with a 1.9 kcal/mol higher enthalpy barrier as compared to that of **1**. The calculations reproduce remarkably well the experimentally obtained rate enhancement for the reaction of **3** and MA having a 5.1 kcal/mol lower enthalpy barrier than that of **1**. The enthalpy barrier for the cycloaddition of **4** is predicted to be comparable to that of **1**.

Finally, this work has pointed out the limitations of the previously proposed models for the diastereoselectivity of chiral anthracene templates and has allowed us to propose new models based on the energy differences between the diastereomeric transition states and their geometries.

Supporting Information Available: Absolute energies, Cartesian coordinates, Mulliken charges, NBO analysis results, and complete ref 16. This material is available free of charge via the Internet at http://pubs.acs.org.